Efficient description of strongly correlated electrons with mean-field cost

Katharina Boguslawski, Paweł Tecmer, and Paul W. Ayers[*]

Department of Chemistry and Chemical Biology, McMaster University, 1280 Main Street West, Hamilton, Ontario, Canada L8S 4M1

Patrick Bultinck

Department of Inorganic and Physical Chemistry, Ghent University, Krijgslaan 281 (S3), 9000 Gent, Belgium

Stijn De Baerdemacker and Dimitri Van Neck[†]

Center for Molecular Modelling, Ghent University, Technologiepark 903, 9052 Gent, Belgium

We present an efficient approach to the electron correlation problem that is well suited for strongly interacting many-body systems, but requires only mean-field-like computational cost. The performance of our approach is illustrated for one-dimensional Hubbard rings with different numbers of sites, and for the nonrelativistic quantum-chemical Hamiltonian exploring the symmetric dissociation of the H_{50} hydrogen chain.

The accurate description of the electron-electron interaction at the quantum-mechanical level is a key problem in condensed matter physics and quantum chemistry. Since most of the quantum many-body problems are extraordinarily difficult to solve exactly, different approximation schemes emerged [1–5], among which the density matrix renormalization group (DMRG) algorithm [6–8] gained a lot of popularity in both condensed matter physics [7] and quantum chemistry [9–16] over the past decade. Since the DMRG algorithm optimizes a matrix product state wave function, it is optimally suited for one-dimensional (1D) systems, though DMRG studies on higher-dimensional and compact systems have been reported [10,13,15,17]. Yet, novel theoretical approaches are desirable that can accurately describe strong correlation effects between electrons where the dimension of the Hilbert space exceeds the present-day limit of DMRG or general tensor-network approaches [18] allowing approximately 100 sites or 60 (spatial) orbitals, respectively.

Another promising approach, suitable for larger strongly correlated electronic systems, uses geminals (two-electron basis functions) as building blocks for the wave function [19–26]. One of the simplest practical geminal approaches is the antisymmetric product of 1-reference-orbital geminals (AP1roG) [27–29]. Unique among geminal methods, AP1roG can be rewritten as a fully general pair-coupled-cluster doubles wave function [30], i.e.,

$$|\Psi_{\mathrm{AP1roG}}\rangle = \exp\left(\sum_{i=1}^{P}\sum_{a=P+1}^{K} c_i^a a_{a\uparrow}^{\dagger} a_{a\downarrow}^{\dagger} a_{i\downarrow} a_{i\uparrow}\right)|\Phi_0\rangle, \quad (1)$$

where $a_{p\sigma}^{\dagger}$ and $a_{p\sigma}$ ($\sigma = \downarrow,\uparrow$) are the fermionic creation and annihilation operators, and $|\Phi_0\rangle$ is some independent-particle wave function (usually the Hartree-Fock determinant). Indices i and a correspond to virtual and occupied sites (orbitals) with respect to $|\Phi_0\rangle$, P and K denote the number of electron pairs ($P = N/2$ with N being the total number of electrons) and

orbitals, respectively, and $\{c_i^a\}$ are the geminal coefficients. This wave-function ansatz is size extensive and has mean-field scaling, $O(P^2(K - P)^2)$ for the projected Schrödinger equation approach [27].

To ensure size consistency, however, it is necessary to optimize the one-electron basis functions [27], where all nonredundant orbital rotations span the occupied-occupied, occupied-virtual, and virtual-virtual blocks with respect to the reference Slater determinant $|\Phi_0\rangle$. We have implemented a quadratically convergent algorithm: We minimize the energy with respect to the choice of the one-particle basis functions, subject to the constraint that the projected Schrödinger equations for the geminal coefficients hold. Specifically, we use a Newton-Raphson optimizer and a diagonal approximation of the orbital Hessian to obtain the rotated set of orbital expansion coefficients. Our algorithm is analogous to the orbital-optimized coupled-cluster approach [31–33]. Due to the four-index transformation of the electron repulsion integrals, the computational scaling deteriorates to $O(K^5)$. The orbital-optimized AP1roG (OO-AP1roG) approach was implemented in a developer version of the HORTON program package [34].

The half-filled one-dimensional Hubbard Hamiltonian. First, we consider the 1D Hubbard model Hamiltonian with periodic boundary conditions,

$$\hat{H}_{\mathrm{Hub}} = -t\sum_{j,\sigma}(a_{(j+1)\sigma}^{\dagger}a_{j\sigma} + a_{j\sigma}^{\dagger}a_{(j+1)\sigma}) + U\sum_{j} n_{j\uparrow}n_{j\downarrow},$$
$$(2)$$

where the first term represents nearest-neighbor hopping and the second term is the repulsive on-site interaction. The operators $a_{j\sigma}^{\dagger}$ and $a_{j\sigma}$ are again the fermionic creation and annihilation operators on a lattice with sites $j = 1, \ldots, N_{\mathrm{sites}}$, and $n_{j\sigma} = a_{j\sigma}^{\dagger}a_{j\sigma}$ is the local number operator.

Figure 1 shows the differences in total energies obtained for OO-AP1roG with respect to reference data obtained from the solution of the Lieb-Wu equations [35] ($N_{\mathrm{sites}} = 6,10,14,50,122$). OO-AP1roG can reproduce the exact total energies in the limit of zero and infinite (repulsive) on-site interaction. The largest deviations from the exact solution (up

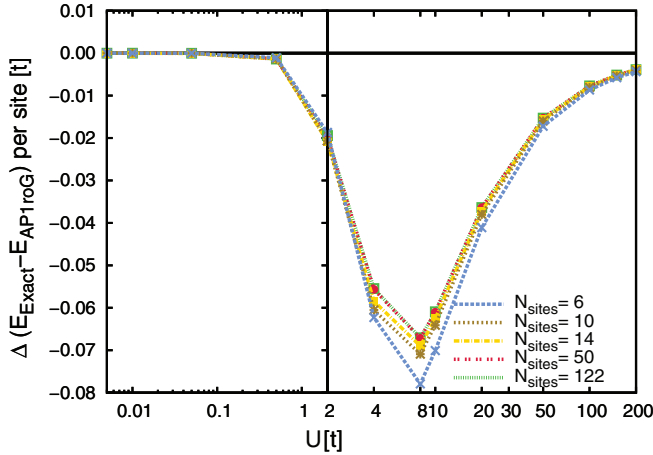―――――――
[*]ayers@mcmaster.ca
[†]dimitri.vanneck@ugent.be

FIG. 1. (Color online) Deviation of the OO-AP1roG total energies from exact values (blue dashed line) for different strengths of the repulsive on-site interaction for the 1D Hubbard model (with periodic boundary conditions) for $N_{sites} = 6, 10, 14, 50, 122$. The exact values for small U ($U < 0.001t$) for $N_{sites} = 50, 122$ could not be converged.

to $0.075t$ per site) are found for the intermediate region of the on-site interaction, that is, for $2t < U < 50t$. Figure 2 shows the percentage of the correlation energy captured by OO-AP1roG calculated as $\%\kappa = \frac{E^{OO\text{-}AP1roG} - E^{HF}}{E^{exact} - E^{HF}} \times 100$. In the limit of zero and infinite U, the OO-AP1roG model becomes exact; for $U = 0$ the wave function can be exactly described by a single Slater determinant and thus the correlation energy approaches zero, while for $U \to \infty$ the quantum state can be represented by the perfect-pairing wave function. For growing (repulsive) U, the percentage of the correlation energy covered by OO-AP1roG increases gradually.

For small values of U, the geminal coefficient matrix $\{c_i^a\}$ is sparse and thus far from perfect pairing, which is represented by a diagonal geminal coefficient matrix (see Fig. 1 in the Supplemental Material [36]). In the limit $U \to 0$, the geminal coefficient matrix correctly approaches the zero matrix,
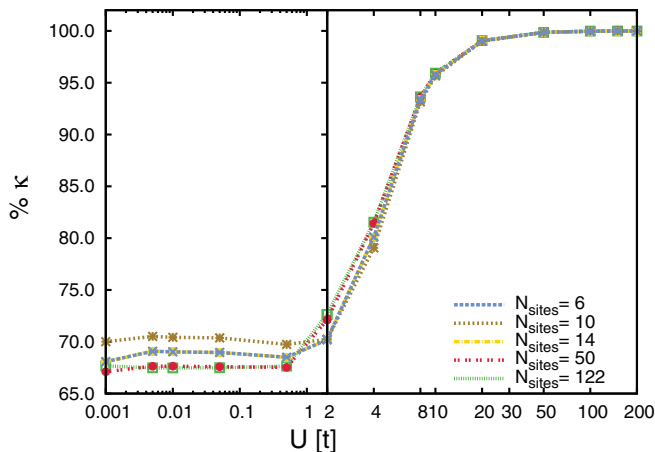

FIG. 2. (Color online) Percentage of the correlation energy $\%\kappa$ for different strengths of the repulsive on-site interaction in the half-filled 1D Hubbard model (with periodic boundary conditions) for $N_{sites} = 6, 10, 14, 50, 122$ captured by OO-AP1roG. The exact values for small U ($U < 0.001t$) for $N_{sites} = 50, 122$ could not be converged.

TABLE I. Spectroscopic constants: equilibrium bond distance (R_e), potential energy depth (D_e), and harmonic vibrational frequency (ω_e) for the ground state of H_{50} (STO-6G). Differences with respect to the DMRG reference data are listed in parentheses.

Method	R_e (Å)	D_e (eV)	ω_e (cm^{-1})
RHF	0.940 (−0.030)	199.0 (+109.3)	25089 (+2268)
AP1roG	0.941 (−0.029)	198.2 (+108.5)	23013 (+2252)
MP2	0.955 (−0.015)	144.1 (+54.4)	24568 (+1747)
PBE	0.971 (+0.001)	146.6 (+56.9)	23662 (+841)
OO-AP1roG	0.966 (−0.004)	82.2 (−7.5)	23013 (+192)
DMRG [40]	0.970	89.7	22821

indicating that a single Slater determinant is sufficient to exactly describe the quantum state. For increasing U, $\{c_i^a\}$ becomes diagonal dominant and adopts a diagonal structure in the limit of $U \to \infty$. Thus, in the limit of infinite (repulsive) interaction, OO-AP1roG optimizes a perfect-pairing (seniority-zero) wave function [37,38],

$$\prod_{i=1,3,\ldots} [(a_{i,\uparrow}^\dagger + a_{i+1,\uparrow}^\dagger)(a_{i,\downarrow}^\dagger + a_{i+1,\downarrow}^\dagger)$$
$$- (a_{i,\uparrow}^\dagger - a_{i+1,\uparrow}^\dagger)(a_{i,\downarrow}^\dagger - a_{i+1,\downarrow}^\dagger)]|0\rangle. \quad (3)$$

To conclude, OO-AP1roG has mean-field-like scaling, but can recover about 71% of the correlation energy in the weak interaction regime, about 80% for intermediate interaction strengths, and approximately 93% in the case of strong on-site interaction for all chain lengths studied (a numerical comparison is presented in Table I of the Supplemental Material).

Figure 3 shows the single-orbital entropy for different lengths of the 1D lattice as a function of the repulsive on-site interaction U. The single-orbital entropy is the analog of the one-site entropy, but determined in the natural orbital basis: It is calculated as the von Neumann entropy from a single-orbital density matrix (a many-particle reduced density matrix of one orbital). It measures the entanglement of one orbital with
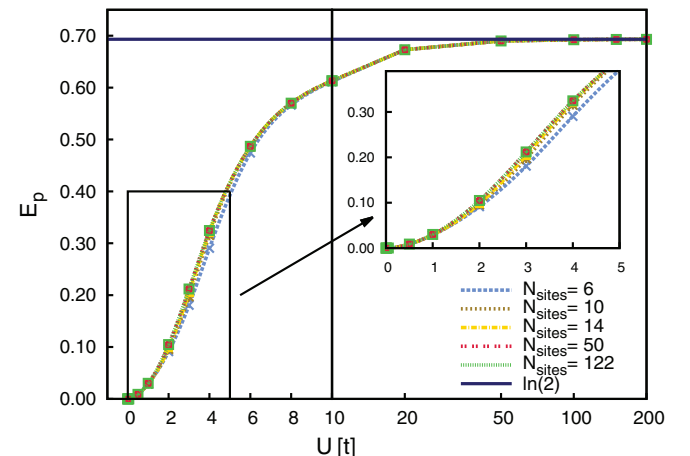

FIG. 3. (Color online) Pair entanglement E_p (single-orbital entropy) for different strengths of the repulsive on-site interaction in the half-filled 1D Hubbard model (with periodic boundary conditions) for $N_{sites} = 6, 10, 14, 50, 122$ calculated by OO-AP1roG.

the remaining ($N_{sites} - 1$) ones [14]. In particular, since the optimized orbitals are localized on two neighboring sites, the von Neumann entropy describes the correlation of a pair of sites and the other part of the system. In the following, we will refer to the single-orbital entropy as the pair entanglement E_p, in accordance with the local entanglement determined for the on-site basis [39].

The pair entanglement takes its minimum value at $U = 0t$, where the wave function can be exactly represented by a single Slater determinant. It is easy to verify that all orbital pairs are uncorrelated in a one-determinant wave function and thus $E_p = 0$. For increasing on-site interaction, the pair entanglement smoothly accumulates (see Fig. 3) and reaches its maximum value of $\ln 2$ in the large U limit (for $U \to \infty$, the single-orbital density matrix has the diagonal elements $\{0,0,0.5,0.5\}$). Note that OO-AP1roG yields similar pair entanglement profiles for all chain lengths studied and correctly reproduces the small and large U limits.

Symmetric dissociation of the H_{50} *molecule.* The nonrelativistic quantum-chemical Hamiltonian in its second quantized form reads

$$\hat{H} = \sum_{pq,\sigma} h_{pq} a_{p\sigma}^\dagger a_{q\sigma}$$
$$+ \frac{1}{2} \sum_{pqrs,\sigma\tau} \langle pq|rs \rangle a_{p\sigma}^\dagger a_{q\tau}^\dagger a_{s\tau} a_{r\sigma} + H_{nuc}, \quad (4)$$

where the first term comprises the kinetic energy and nuclear-electron attraction, the second term is the electron-electron interaction, and the third term represents the nuclear-nuclear repulsion energy, respectively. In Eq. (4), indices p, q, r, and s run over all one-particle basis functions, while σ and τ denote the electron spin ($\{\uparrow,\downarrow\}$). The Hamiltonian as defined in Eq. (4) was used for the study of the symmetric stretching of the H_{50} hydrogen chain, which is a commonly used molecular model for strongly correlated systems and which remains a challenging problem for conventional quantum-chemistry methods [40–43].

In Fig. 4, the performance of AP1roG and OO-AP1roG is compared to restricted Hartree-Fock (RHF), second-order Møller-Plesset (MP2) perturbation theory, coupled-cluster theory with singles, doubles and perturbative triples [CCSD(T)], and density functional theory using the Perdew-Burke-Ernzerhof (PBE) [45] exchange-correlation functional. As a reference, the DMRG potential energy curve determined in Ref. [40] was used, which can be considered as the exact-diagonalization limit. None of the standard quantum chemical methods, such as MP2, CCSD(T), or DFT using the PBE exchange-correlation functional, yield qualitatively correct energy curves for the symmetric stretching of the H_{50} chain. In particular, the potential energy depth determined from DFT and MP2 is too deep, while CCSD(T) does not converge for interatomic distances larger than 2.0 Å. Note that
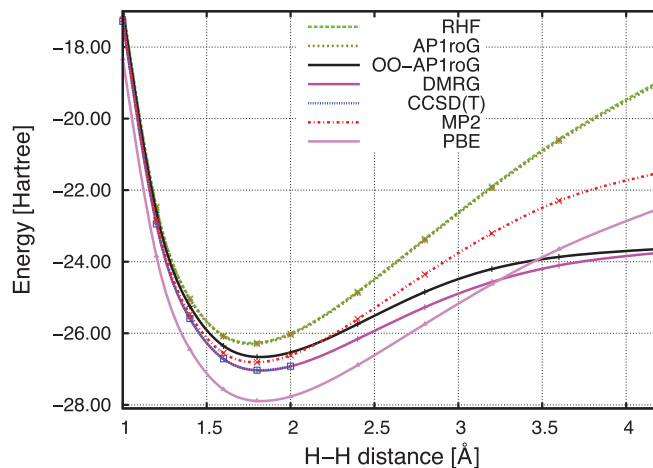

FIG. 4. (Color online) Symmetric dissociation of the H_{50} chain using the STO-6G basis set [44] obtained from different methods. The DMRG reference data are taken from Ref. [40].

the lack of size consistency in AP1roG is cured by orbital optimization in the OO-AP1roG approach. The latter yields a potential energy curve that is closest to the DMRG reference data along the whole dissociation pathway and leads to a proper dissociation limit of H_{50}. Moreover, the OO-AP1roG method gives spectroscopic constants (presented in Table I) that are in excellent agreement with DMRG reference data, outperforming standard quantum-chemistry approaches.

Wave functions constructed as antisymmetric products of nonorthogonal geminals, such as the AP1roG wave function scrutinized here, provide an alternative approach to electronic structure, with mean-field scaling. Because it uses electron pairs as a building block, AP1roG is a suitable way to describe strong correlations dominated by electron pairing. However, in order to ensure size consistency, the single-particle (orbital) basis used to construct the electron pairs must be optimized. Our results show that orbital-optimized AP1roG is a robust method all the way from the weakly correlated to the strongly correlated limit, in both molecules and periodic systems.

[1] W. Foulkes, L. Mitas, R. Needs, and G. Rajagopal, Rev. Mod. Phys. **73**, 33 (2001).

[2] D. I. Lyakh, M. Musiał, V. F. Lotrich, and R. J. Bartlett, Chem. Rev. **112**, 182 (2012).

[3] G. K.-L. Chan and S. Sharma, Annu. Rev. Phys. Chem. **62**, 465 (2011).

[4] L. Pollet, Rep. Prog. Phys. **75**, 094501 (2012).

[5] R. Rodríguez-Guzmán, C. A. Jiménez-Hoyos, R. Schutski, and G. E. Scuseria, Phys. Rev. B **87**, 235129 (2013).

[6] S. R. White, Phys. Rev. Lett. **69**, 2863 (1992).

[7] U. Schollwöck, Rev. Mod. Phys. **77**, 259 (2005).

[8] O. Legeza, R. M. Noack, J. Sólyom, and L. Tincani, in *Computational Many-Particle Physics*, edited by H. Fehske, R. Schneider, and A. Weiße, Lecture Notes in Physics Vol. 739 (Springer, Berlin, 2008), pp. 653–664.

[9] K. H. Marti and M. Reiher, Z. Phys. Chem. **224**, 583 (2010).

[10] K. Boguslawski, K. H. Marti, O. Legeza, and M. Reiher, J. Chem. Theory Comput. **8**, 1970 (2012).

[11] K. Boguslawski, P. Tecmer, O. Legeza, and M. Reiher, J. Phys. Chem. Lett. **3**, 3129 (2012).

[12] S. Wouters, P. A. Limacher, D. Van Neck, and P. W. Ayers, J. Chem. Phys. **136**, 134110 (2012).

[13] Y. Kurashige, G. K.-L. Chan, and T. Yanai, Nat. Chem. **5**, 660 (2013).

[14] K. Boguslawski, P. Tecmer, G. Barcza, O. Legeza, and M. Reiher, J. Chem. Theory Comput. **9**, 2959 (2013).

[15] P. Tecmer, K. Boguslawski, O. Legeza, and M. Reiher, Phys. Chem. Chem. Phys. **16**, 719 (2014).

[16] S. Wouters, W. Poelmans, P. W. Ayers, and D. Van Neck, Comput. Phys. Commun., doi:10.1016/j.cpc.2014.01.019 (2014).

[17] M. C. Chung and I. Peschel, Phys. Rev. B **62**, 4191 (2000).

[18] V. Murg, F. Verstraete, O. Legeza, and R. M. Noack, Phys. Rev. B **82**, 205105 (2010).

[19] A. C. Hurley, J. Lennard-Jones, and J. A. Pople, Proc. R. Soc. London, Ser. A **220**, 446 (1953).

[20] A. J. Coleman, J. Math. Phys. **6**, 1425 (1965).

[21] D. M. Silver, J. Chem. Phys. **50**, 5108 (1969).

[22] J. V. Ortiz, B. Weiner, and Y. Ohrn, Int. J. Quantum Chem. **20**, 113 (1981).

[23] P. R. Surjan, in *Correlation and Localization* (Springer, Berlin, 1999), pp. 63–88.

[24] W. Kutzelnigg, Chem. Phys. **401**, 119 (2012).

[25] P. R. Surján, A. Szabados, P. Jeszenszki, and T. Zoboki, J. Math. Chem. **50**, 534 (2012).

[26] J. K. Ellis, R. L. Martin, and G. E. Scuseria, J. Chem. Theory Comput. **9**, 2857 (2013).

[27] P. A. Limacher, P. W. Ayers, P. A. Johnson, S. De Baerdemacker, D. Van Neck, and P. Bultinck, J. Chem. Theory Comput. **9**, 1394 (2013).

[28] P. Limacher, P. Ayers, P. Johnson, S. De Baerdemacker, D. Van Neck, and P. Bultinck, Phys. Chem. Chem. Phys. **16**, 5061 (2014).

[29] P. A. Limacher, T. D. Kim, P. W. Ayers, P. A. Johnson, S. De Baerdemacker, D. Van Neck, and P. Bultinck, Mol. Phys. **112**, 853 (2014).

[30] T. M. Henderson, J. Dukelsky, G. E. Scuseria, A. Signoracci, and T. Duguet, arXiv:1403.6818.

[31] T. Helgaker, P. Jørgensen, and J. Olsen, *Molecular Electronic-Structure Theory* (Wiley, New York, 2000).

[32] G. E. Scuseria and H. F. Schaefer III, Chem. Phys. Lett. **142**, 354 (1987).

[33] U. Bozkaya, J. M. Turney, Y. Yamaguchi, H. F. Schaefer, and C. D. Sherrill, J. Chem. Phys. **135**, 104103 (2011).

[34] T. Verstraelen, S. Vandenbrande, M. Chan, F. H. Zadeh, C. Gonzalez, K. Boguslawski, P. Tecmer, P. A. Limacher, A. Malek, HORTON 1.2.0 2013, http://theochem.github.com/horton/.

[35] E. H. Lieb and F. Y. Wu, Phys. Rev. Lett. **20**, 1445 (1968).

[36] See Supplemental Material at http://link.aps.org/supplemental/10.1103/PhysRevB.89.201106 for Geminal matrix coefficient, ground-state and correlation energies for the one-dimensional Hubbard model.

[37] E. Neuscamman, Phys. Rev. Lett. **109**, 203001 (2012).

[38] L. Bytautas, T. M. Henderson, C. A. Jiménez-Hoyos, J. K. Ellis, and G. E. Scuseria, J. Chem. Phys. **135**, 044119 (2011).

[39] S.-J. Gu, S.-S. Deng, Y.-Q. Li, and H.-Q. Lin, Phys. Rev. Lett. **93**, 086402 (2004).

[40] J. Hachmann, W. Cardoen, and G. K.-L. Chan, J. Chem. Phys. **125**, 144101 (2006).

[41] T. Tsuchimochi and G. E. Scuseria, J. Chem. Phys. **131**, 121102 (2009).

[42] L. Stella, C. Attaccalite, S. Sorella, and A. Rubio, Phys. Rev. B **84**, 245117 (2011).

[43] N. Lin, C. A. Marianetti, A. J. Millis, and D. R. Reichman, Phys. Rev. Lett. **106**, 096402 (2011).

[44] W. J. Hehre, R. F. Stewart, and J. A. Pople, J. Chem. Phys. **51**, 2657 (1969).

[45] J. P. Perdew, K. Burke, and M. Ernzerhof, Phys. Rev. Lett. **77**, 3865 (1996).